catalysts

MDPI

Article

Cr-Phthalocyanine Porous Organic Polymer as an Efficient and Selective Catalyst for Mono Carbonylation of Epoxides to Lactones

Vinothkumar Ganesan and Sungho Yoon *

Department of Chemistry, Chung-Ang University, 84, Heukseok-ro, Dongjak-gu, Seoul 06974, Korea; vinothcau@cau.ac.kr

* Correspondence: sunghoyoon@cau.ac.kr

Received: 19 July 2020; Accepted: 6 August 2020; Published: 8 August 2020

Abstract: A facile, one-pot design strategy to construct chromium(III)-phthalocyanine chlorides (Pc'CrCl) to form porous organic polymer (POP-Pc'CrCl) using solvent knitting Friedel-Crafts reaction (FCR) is described. The generated highly porous POP-Pc'CrCl is functionalized by post-synthetic exchange reaction with nucleophilic cobaltate ions to provide an heterogenized carbonylation catalyst (POP-Pc'CrCo$(CO)_4$) with Lewis acid-base type bimetallic units. The produced porous polymeric catalyst is identical to that homogeneous counterpart in structure and coordination environments. The catalyst is very selective and effective for mono carbonylation of epoxide into corresponding lactone and the activities are comparable to those observed for a homogeneous Pc'CrCo$(CO)_4$ catalyst. The (POP-Pc'CrCo$(CO)_4$) also displayed a good catalytic activities and recyclability upon successive recycles.

Keywords: Cr-phthalocyanine; porous organic polymer; Friedel–Crafts reaction; heterogeneous catalysis; carbonylation; β-lactones; catalyst recyclability

1. Introduction

β-Lactones are an important class of energetically favored four-membered heterocycles with prevalent utilities in the chemical industry, since they are crucial intermediates for the production of various derivatives of β-hydroxy acids, biodegradable poly(β-hydroxyalkanotes), succinic anhydrides, and acrylic acids [1–9]. Their inherent ring strain facilitates excellent reactivity, allowing them to undergo a range of transformations to provide products with a variety of applications ranging from polymer chemistry to natural product synthesis [4]. However, synthetic routes to β-lactones are limited. Recently, ring-expansion epoxide carbonylation utilizing inexpensive C1 sources have emerged as a convenient and direct method to produce β-lactones with good atom economy [10].

Although there have been numerous reports of ring-expansion carbonylation catalysts, well-defined Lewis acid–base ion pairing catalysts of the common type [Lewis acid]$^+$ $[Co(CO)_4]^-$ have demonstrated high efficiency for these transformations [11–13]. Among the reported Lewis acid–base pair catalysts, the porphyrin-based $[OEPCr(THF)_2]^+$ $[Co(CO)_4]^-$ (OEP = Octaethylporphyrinato, THF = tetrahydrofuran) catalyst has demonstrated high reactivity and high selectivity toward mono carbonylation under homogeneous conditions [14]. However, tedious catalyst synthesis and product separation have limited the use of this catalytic system and motivated the search for viable alternatives, including heterogeneous systems [15–17]. In addition to the heterogenization of catalysts to improve recyclability, facile synthesis of such catalytic systems is being actively researched [18–20].

Phthalocyanine (Pc), which is a porphyrinoid analogue, is easily synthesized with excellent yields and could serve as an alternative for porphyrin systems; because of their planar tetradentate dianionic

ligation, phthalocyanines are excellent structural analogs to porphyrins and are synthetically facile. Recently, we demonstrated that a catalyst generated in situ from commercial (AlPcCl) and $Co_2(CO)_8$ displayed excellent activity for mono and double carbonylation [21]. But, the selectivity toward β-lactones was very poor, hence, Lewis acidic Al^{3+} containing [Lewis acid]$^+$ $[Co(CO)_4]^-$ type ion pairing catalysts are proven to be active also for double carbonylation and generally resulting in a mixture of β-lactones and anhydrides [3,21,22]. Therefore, Cr^{3+} containing [PcCr(III)]$^+$ $[Co(CO)_4]^-$ type catalyst could be a suitable Lewis acidic part for selective monocarbonylation of epoxides into β-lactones [12,13,23]. However, partial solubility of Pc metal complex due to intermolecular π–π stacking interactions leads to reduced collision between the Pc metal complex and substrate (epoxide) resulting in low catalytic activity. These enforced further structural tunings on the Pc ring to improve the catalyst solubility and activity by controlling such a π–π stacking interactions; in addition, the intensely colored Pc metal complexes were difficult to separate from the reaction mixture [21,24,25].

Immobilization of soluble Pc metal complexes on a flexible POP addresses both, solubility and separation issues, by providing a heterogeneous catalytic system. In this regard, we strategically designed and synthesized a new phthalocyanine chromium(III) chloride complex (Pc'Cr(III)Cl) and heterogenized using a simple, one-pot solvent-knitting Friedel–Crafts reaction (FCR); the resulting complex was functionalized with $[Co(CO)_4]^-$ anion to generate a highly active and recyclable [POP-Pc'Cr(III)]$^+$ $[Co(CO)_4]^-$ catalytic system.

2. Results and Discussion

2.1. Synthesis and Characterization of POP-Pc'Cr(III)Cl

A synthetic strategy of POP-Pc'Cr(III)$Co(CO)_4$ (**4**) is shown in Scheme 1. At first, the ligand **1** is synthesized by the mild base-catalyzed condensation [26]. The monomer Pc'Cr(III)Cl (**2**) was synthesized with excellent yield according to the modified literature procedure and characterized by FTIR and UV-Visible spectroscopic techniques, further confirmed by high-resolution mass spectrometry as shown in Figures S1–S4 [27,28]. The substituted 2-isopropylphenolic group not only improves the solubility of the monomer **2** but also acts as a knitting group through covalent linkages by $AlCl_3$-catalyzed FCR using methylene dichloride both as a crosslinker and as a solvent. The resulting dark green color porous organic polymer POP-Pc'CrCl (**3**) is stable under open atmosphere conditions and not soluble in most commonly used organic solvents as a result of extensive cross-linking [18,19]. The compositional homogeneity and the surface topography of POP **3** was probed by a scanning electron microscope (SEM) and a transmission electron microscope (TEM) analysis. Figure 1a,b shows the SEM and TEM images of **3** respectively, as an aggregate of polydisperse spherical shape particles of 1 μm size average (Figures S5 and S6). Energy dispersive X-ray (EDS) analysis shows the relative abundance of constituent elements throughout the Pc' polymeric matrix indicating uniform distribution of elements after polymerization (Figure S5) [29]. A powder X-ray diffraction analysis of the resulting polymer showed that a wide peak at $2\theta = 13.1°$ attributes to the construction of amorphous polymeric material (Figure S7a). Subsequently, the absence of distinctive sharp monomeric diffraction peaks (Figure S7b) suggests that the solvent knitting polymerization is thoroughly completed and the resulting POP is free from crystalline monomer residues [18]. The thermal endurance of the resulting polymeric material was characterized by thermogravimetric analysis (TGA) as shown in Figure S8, the polymeric material was stable up to 400 °C indicating possible outstanding thermal stability under harsh reaction conditions.

The porosity of POP-Pc'CrCl, **3** was investigated by N_2 sorption measurement carried out at 77 K. The Pc'-based polymer **3** exhibited characteristic type-I adsorption isotherms (as per IUPAC adsorption isotherms classification), as depicted in Figure 1c [30]. A steep N_2 uptake at a lower relative pressure (P/P_0 = 0–0.1) region is attributed to the microporous character of polymer **3**, whereas the hysteresis loop behavior throughout the range of relative pressure can be attributed to the existence of mesoporosity. The BET (Brunauer–Emmett–Teller) surface area of the polymeric material is 725 $m^2\ g^{-1}$

and the total pore volume is 0.388 cm^3 g^{-1} (Figure 1c and Figure S9a). These porosity results are comparable with other reported Pc-based porous polymers and indicate high surface area, which enables larger exposure of active sites per unit mass of the material; they also confirm the distribution of high grade porous structure that can accommodate bulky functional groups via the labile chloro ligand for specific catalytic applications [18,31–33].

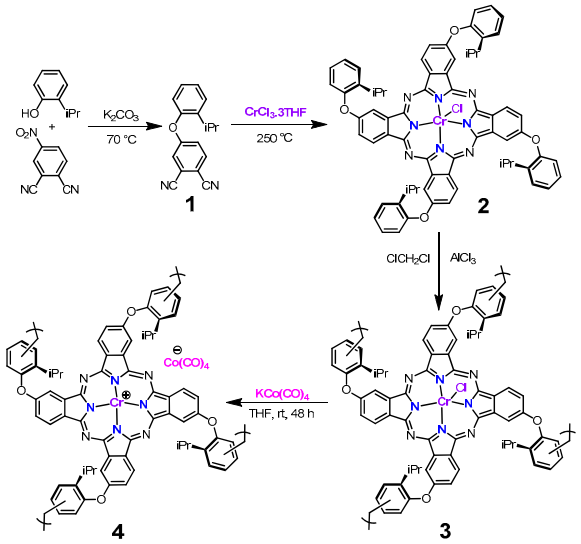

Scheme 1. Synthesis of catalyst 4 by the Friedel-Crafts reaction (FCR).

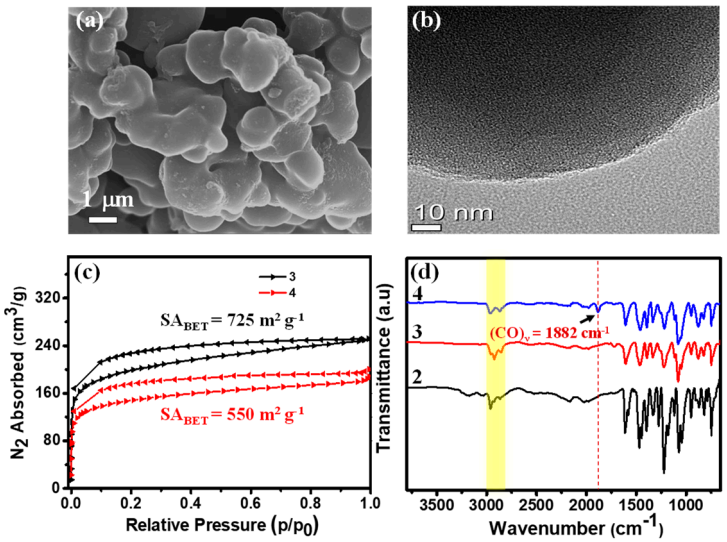

Figure 1. (**a**) SEM image of POP-Pc'CrCl, (**b**) TEM image of **3**, (**c**) N_2 sorption isotherms of **3** and **4** at 77 K, and (**d**) FTIR spectra of **2**, **3**, and **4**.

The chemical structure of the resulting polymer was analyzed using FTIR spectroscopy. Comparative FTIR spectral analysis of the monomeric complex and the formed porous polymer was performed to evaluate the structural integrity of the resulting polymers, as displayed in Figure 1d. IR peaks appearing in the range of 3068–2856 cm^{-1} are attributed to −C=C−H stretching vibrations of the aromatic functional groups of the phthalocyanine complex and polymer **3**, as well as to the newly formed methylene crosslinking bridges [34]. The peaks at 1610, 1470, and 1390 cm^{-1} can be assigned for C=C, C–N, and C=N stretching vibrations, respectively, of the Pc' ring, which contains benzene, aza, and pyrrole functional groups; these are present in the formed polymers as well as the parent monomers [31,35,36]. These FTIR spectroscopic analysis shows that the resulting POP retains most

of the feature peaks of its corresponding monomer and is consistent with the anticipated polymeric structure. Thus, these analysis results unambiguously verify the direct heterogenization of Pc'Cr(III)Cl complex by the one-pot FCR to produce very stable, and heterogeneous porous polymeric materials.

2.2. Synthesis and Characterization of POP-Pc'Cr(III)Co(CO)$_4$

Heterogeneous phthalocyanine polymer matrix is a probable candidate for Lewis-acid-enabled catalytic transformations. Particularly, the Pc'Cr(III)Cl complex resembles TPPCr(III)Cl (TPP = Tetraphenylporphyrinato), the best candidate for the carbonylation of epoxides with an additional Lewis base incorporation [13,37]. Interestingly, polymeric material **3** can be incorporated with an appropriate base via its labile Cl^- anions in order to form a Lewis acid–base ion pair catalyst [12–14]. Accordingly a metathesis reaction of $Co(CO)_4^-$ anions can replace the labile Cl^- ions to generate a heterogeneous bimetallic frustrated Lewis acid-base ion pair type catalyst ([Lewis acid]$^+$[Co(CO)$_4$]$^-$)to promote the epoxide ring-expansion carbonylation [17–20]. As such, polymer **3** was treated with excess $KCo(CO)_4$ to generate the heterogeneous epoxide carbonylation catalyst [POP-Pc'Cr]$^+$ [Co(CO)$_4$]$^-$ (**4**) [12–14]. At first the resulting catalyst **4** was characterized by FTIR spectroscopic technique. Compared to polymer **3** (contains Cl^-), the $Co(CO)_4^-$ anions exchanged catalyst **4** exhibits a strong new absorption peak at 1882 cm^{-1} (Figure 1d). This peak is characteristic of typical ν(CO) from newly exchanged tetrahedral $Co(CO)_4^-$ ions, consistent with that of previously reported well-defined homogeneous Cr-containing [Lewis acid]$^+$ [Co(CO)$_4$]$^-$-type catalysts [17,19]. SEM and TEM images of the catalyst indicate no morphology change after $Co(CO)_4^-$ anion exchange. Subsequently, EDS analysis confirms the incorporation of Co into the polymeric frameworks along with other constituent elements, distributed uniformly all over the polymer(Figure 2a,b, Figures S10 and S11). Atomic absorption spectroscopy (AAS) and inductively coupled plasma–optical emission spectroscopy (ICP-OES) revealed that the Co and Cr contents were 1.78 and 3.63 wt%, respectively, against, 4.63 and 4.09 wt% calculated for Co and Cr, respectively, in well-defined homogeneous catalyst. The molar ratio of the Cr/Co content in catalyst **4** is 1.8 (determined by ICP-AAS), indicating partial exchange of Cl^- ion and a part of Lewis-acidic Cr^{3+} remains combined with Cl^- ions; they could be buried inside the microporous channels and/or inaccessible for cobaltate exchange. Limited molecular exchange of cobaltate ion pairs is consistent with SEM-EDS analysis and also reported previously [17,19].

The coordination environment of the catalyst **4** metal species was characterized using X-ray photoelectron spectroscopy (XPS). The XPS peak for Cr *2p* shows a characteristic doublet at 577.21 and 586.70 eV as shown in Figure 2c, which matches well with the structural analogues, the POP-TPP-supported Cr(III) species, and analogous metal center on porous organic networks [17,19,20,38]. As shown in Figure 2d, the XPS peaks for Co species are detected at 796.90 eV and 781.55 eV along with the typical shoulder is for the Co $2p_{1/2}$ and Co $2p_{3/2}$ orbitals of the $Co(CO)_4^-$ species, respectively. The observed Co XPS peaks values are also consistent with those of $Co(CO)_4^-$-exchanged similar TPPAl, CTF-Al(OTf), and TPPCr heterogeneous catalysts [16–20]. Finally, the porosity retention is evident from TEM images (Figure S11) and N_2 gas sorption measurements carried out at 77 K, which afford type-I isotherms and exhibiting hysteresis loop behavior, displaying a combination of micro and mesoporosity (Figure 1c). However, the BET surface area is reduced to 550 m^2 g^{-1} for catalyst **4,** and a decreased total pore volume of 0.28 cm^3 g^{-1} (related to the parent polymeric network) is observed (Figure 1c and Figure S9b). This suggests that the exchanged $Co(CO)_4^-$ anions partly occupy the porous channels of polymeric network, thereby decreasing the total available pore volume as observed previously [17–19]. Nevertheless, the catalyst maintains a porous structure to allow the substrate epoxide and the product β-butyrolactone molecules to diffuse over the Lewis acid–base-ions paired porous channels.

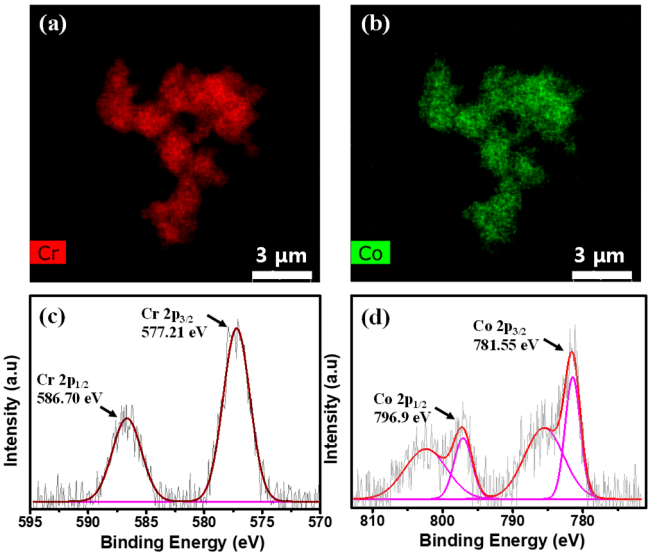

Figure 2. STEM-EDS mapping image of (**a**) Cr atoms and (**b**) Co atoms and X-ray photoelectron profiles of **4** for deconvoluted (**c**) Cr2*p* and (**d**) Cobalt *2p* core level.

2.3. Carbonylation Activity of POP-Pc'Cr(III)Co(CO)$_4$

Catalyst **4** was tested for carbonylation catalytic activity in a 50 mL stainless steel custom-made one inch tubular reactor. Propylene oxide (PO) was used as an epoxide substrate with CO under 6 MPa pressure. Various solvents were tested, since carbonylation is affected by the type of solvent [14,22]. The crude reaction mass was analyzed by ^{1}H NMR spectral analysis using an internal standard naphthalene; the results are summarized in Table 1. Among the solvents screened, weakly coordinating DME is the most active solvent system for PO carbonylation to β-butyrolactone with >99% conversion and selectivity (entries 1–4), consistent with earlier reports for POP-TPPCrCo(CO)$_4$ and analogs [17,19,20]. Using similar reaction conditions, we evaluated the catalytic activity of homogenous well-defined [Pc'Cr][Co(CO)$_4$]; we observed conversion of >99% and selectivity of 99% toward β-butyrolactone (entry 5). The activity was tested with a higher PO ratio, and the yield was reduced to a ratio of 200 (entry 6). Reactions were performed for 12 h and 1 h under same reaction conditions (entry 7 and 8, respectively) to get initial rates of conversion, and the carbonylation yields of 70 and 22% were observed, respectively, with a site time yield of 44 h^{-1}. Finally, the activity was tested at room temperature; 40% yield was achieved with a substrate/catalyst ratio of 100 (entry 9). The activity of POP-Pc'Cr(III)Cl was also evaluated under the same reaction conditions; we observed only PO to polyether conversion, owing to the absence of a Lewis base for carbonyl group insertion (entry 10) [21].

Table 1. Carbonylation activity of catalyst 4.

Entry [a]	Catalyst	Solvent	Epoxide/Co Ratio [b]	T (°C)	Time (h)	Yield [c] (%)	Lactone (%)	Acetone (%)
1	4	DME	200	60	24	>99	>99	<1
2	4	THF	200	60	24	50	99	1
3	4	1,4-dioxane	200	60	24	52	>99	<1
4	4	Toluene	200	60	24	75	>99	<1
5	[Pc'Cr][$Co(CO)_4$]	DME	200	60	24	>99	99	1
6	4	DME	400	60	24	52	>99	<1
7	4	DME	200	60	12	70	>99	<1
8	4	DME	200	60	1	22	>99	<1
9	4	DME	100	30	24	40	>99	trace
10	3	DME	200	60	24	12 [d]		

[a] Reactions performed in DME solution of epoxide (1.8 M) under 6 MPa CO pressure at respective temperature. The mixture was stirred in a preheated oil bath to maintain respective temperature. [b] Calculated based on ICP-AAS value for Co content. [c] Determined by ^{1}H-NMR spectra with an internal standard naphthalene. [d] Polyether was formed.

Before testing recyclability, the heterogeneous nature of catalyst **4** was examined using a hot filtration test; a suspension of catalyst **4** in DME solvent was stirred at 60 °C for 6 h, and the treated catalyst was separated by filtration [15,18]. The dried solid catalyst and filtrate were subjected to the standard carbonylation conditions (2 mol% of catalyst, 6 MPa of CO, 60 °C, and 24 h reaction time) separately. Only the separated solids promoted epoxide carbonylation: no significant epoxide conversion was observed in the presence of the filtrate under the same conditions. This confirms that catalyst **4** retains heterogeneity [18,19]. Finally, catalyst **4** was evaluated for recyclability. Epoxide carbonylation was carried out with catalyst **4** at 30 °C temperature for 24 h under 6 MPa CO pressure in DME solvent. After the reaction, the reaction mixture was filtered inside a glove box to isolate the solid catalyst, which was then washed with dry DME and dried under vacuum; the dried catalyst was used for successive cycles. ^{1}H NMR spectral analysis of the recovered filtrate was conducted to evaluate the recycling ability of the catalyst, as listed in Table 2. The activity was reduced from complete conversion to 98% in the second cycle. The activity decreased further to 85 ± 6% in the third cycle. After the third cycle, the catalyst was analyzed by SEM-EDS to understand the reason for the decreased activity. SEM-EDS analysis of catalyst **4** after third cycle shows no changes in the catalyst morphology, but did reveal an increase in the Cr/Co ratio due to reduced Co content in the catalyst. As shown in Figure S12, the ratio of Cr/Co increased from 1.8:1 to 3.5:1 after the third cycle [16–19]. This suggests that the decreased Co content in the catalyst causes reduced activity during recycling [18,19]. Notably, the spent catalyst (after three cycles) was subjected to treatment with $KCo(CO)_4$ for regeneration [17–19]. The regenerated catalyst revealed restoration of the catalytic activity upon testing. This further substantiates that leaching of Co causes catalyst deactivation during recycling and the catalyst activity can be restored by treating with cobaltate ions to replenish the activity. Thus, POP-Pc'Cr$Co(CO)_4$, prepared via the solvent-knitting FCR, is an efficient and recyclable heterogeneous catalyst.

Table 2. Recyclability of **4.**

Cycle	Yield (%)	Selectivity (%)
		β-Butyrolactone/Acetone
1	>99	>99/<1
2	98	>99/<1
3	85 ± 6	>99/<1
4 *	98	>99/<1

Reaction conditions: catalyst 2 mol%, 6 MPa of CO pressure, 30 °C, DME solvent. The PO conversion was determined by ^{1}H NMR spectra measured with internal standard naphthalene. * regenerated catalyst.

3. Experimental Section

3.1. Materials and Methods

All chemicals and reagents were procured from commercial dealers and used as received unless otherwise mentioned. Chemicals 4-nitrophthalonitrile, 2-isopropylphenol, anhydrous aluminum chloride ($AlCl_3$), dicobaltoctacarbonyl ($Co_2(CO)_8$), tetrahydrofuran (THF), dimethanoxyethane (DME), 1,4-dioxane, toluene, and propylene oxide (PO) were purchased from Sigma-Aldrich (Seoul, Korea). The solvent THF, DME, 1,4-dioxane, and toluene were distilled over sodium/benzoquinone and PO was distilled over CaH_2 under argon atmosphere. Deuterated solvents were purchased from Cambridge Isotope Laboratories, Inc. (T&J Tech Inc, Seoul, Korea). Research grade carbon monoxide was purchased from Air Liquide Korea Co., Ltd. (Seoul, Korea) with 99.998% purity and used as received. The $KCo(CO)_4$ was synthesized according to the reported procedure [39,40]. All manipulations of air and moisture sensitive compounds were carried out inside the glove box under argon atmosphere. Attenuated total reflectance infrared (ATR-IR) measurements were carried out on a Nicolet iS 50 (Thermo Fisher Scientific, Waltham, MA, USA). Scanning electron microscopy (SEM) and energy-dispersive spectroscopy (EDS) measurements were performed using a JEM-7610F (JEOL Ltd., Tokyo, Japan) operated at an accelerating voltage of 20.0 kV. The morphology of the prepared catalysts was observed by a transmission electron microscope Tecnai G2 (FEI Company, Hillsboro, OR, USA). TEM-EDX elemental mapping was obtained with transmission emission microscopy Talos F200X (Thermo Fisher Scientific, Waltham, MA, USA). The X-ray photoelectron spectrum (XPS) was obtained using K-Alpha X-ray photoelectron spectrometer (Thermo Fisher Scientific, Waltham, MA, USA). The binding energies were corrected by the C1s peak from carbon contamination to 284.6 eV. The metal content of the catalysts was analyzed by inductively coupled plasma optical emission spectroscopy (ICP-OES) (iCAP 6000 series, Thermo Fisher Scientific, Waltham, MA, USA) using a microwave-assisted acid digestion system (MARS6, CEM/USA). Samples (~20.0 mg) were digested in a mixture of conc. HCl (20.0 mL) and conc. H_2SO_4 (10.0 mL) solution under microwave rays at 210 °C for 60 min (ramp rate = 7 °C/min). N_2 adsorption-desorption measurements were conducted in an automated gas sorption system (Belsorp II mini, MicrotracBEL, Osaka, Japan) at 77 K; the samples were degassed for 12 h at 80 °C before the measurements. The Brunauer-Emmett-Teller (BET) and Barrett-Joyner-Halenda (BJH) methods were used for calculating the surface areas and pore size distributions, respectively. Powder X-ray diffraction (PXRD) was measured on a RIGAKU D/Max 2500 V using CuKα radiation. ^{1}H and ^{13}C NMR were measured on a 600 MHz Varian VNS NMR spectrometer (Varian, Inc., CA, USA) and 400 MHz NMR spectrometer Bruker Avance III 400 (Bruker Korea Co., Ltd., Seoul, Korea). Simultaneous DSC-TGA instrument (TA instruments, New Castle, DE, USA) was used for the thermogravimetric analysis (TGA) with a heating rate of 10 °C/min from 25 °C to 800 °C under nitrogen atmosphere. UHR-MS measurements were performed on Bruker compact mass spectrometer (Bruker Korea Co., Ltd., Seoul, Korea).

3.2. Synthesis of Pc′ Ligand

4-Nitrophthalonitrile (5.01 g, 0.03 mol), 2-isopropylphenol (4.34 g, 0.03 mol), and K_2CO_3 (6.00 g, 0.04 mol) were stirred in anhydrous *N*,*N*-dimethylformamide (20 mL) at 52 °C for 24 h under N_2 atmosphere. A dark brown solution was obtained and was poured into ice-cold water (200 mL). The resulting brown precipitate was filtered, washed with water, and dissolved in dichloromethane (200 mL); the organic phase was purified by water extraction (3 × 100 mL). The desired product was purified by flash column chromatography (silica gel; hexane/ethyl acetate: 10:1) and recrystallized in hot methanol to obtain a pale white crystalline solid in 90% yield. FTIR: (cm^{-1}) 3085, 2977, 2870, 2233, 1590, 1481, 1446, 1415. 1311, 1280, 1246, 1218, 1184, 1084, 952, 872, 852, 775, 752; ^{1}H NMR (600 MHz, $CDCl_3$, ppm) δ 7.71 (d, *J* = 8.7 Hz, 1H), 7.42 (dd, *J* = 7.5, 1.8 Hz, 1H), 7.32–7.25 (m, 2H), 7.23 (d, *J* = 2.5 Hz, 1H), 7.18 (dd, *J* = 8.7, 2.6 Hz, 1H), 6.93 (dd, *J* = 7.8, 1.3 Hz, 1H), 3.03 (dt, *J* = 13.8, 6.9 Hz, 1H), 1.18 (d, *J* = 6.9 Hz, 6H).^{13}C NMR (151 MHz, $CDCl_3$) δ 162.33 (s), 150.63 (s), 140.91 (s), 135.56 (s), 128.14 (s), 127.90 (s), 127.05 (s), 121.08 (s), 121.03 (s), 120.85 (s), 117.84 (s), 115.55 (s), 115.13 (s), 108.65 (s), 27.34 (s), 23.15 (s).

3.3. Synthesis of Pc′Cr(III)Cl

In a glove box, $CrCl_3$·3THF (0.36 g, 0.96 mmol) and 4-(2-isopropylphenoxy)phthalonitrile (1.00 g, 3.82 mmol) were added to a 20 mL ampoule, which was then sealed under high vacuum. The ampoule was heated at a rate of 60 °C per hour to 250 °C and maintained at the same temperature for 5 h. The ampoule was then cooled to room temperature to obtain a dark product. The product was subsequently removed from the ampoule and purified by Soxhlet extraction using dichloromethane for 48 h to obtain a very dark green crystalline product in 80% yield. FTIR: (cm^{-1}) 3174, 2962, 2865, 1612, 1470, 1396, 1334, 1276, 1222, 1072, 1045, 952, 872, 818, 790, 748; UV-Vis: (THF) λ_{max} 281, 366, 491, 622, 690 nm; HRMS (ESI Q-TOF) m/z calculated $[C_{68}H_{56}CrN_8O_4]^+$ 1100.3830, found [M-Cl]$^+$ 1100.3832.

3.4. Synthesis of POP-Pc′Cr(III)Cl

Under Ar atmosphere, Pc′Cr(III)Cl (1.00 g, 0.87 mmol) was suspended in 40 mL dichloromethane, the reaction mixture was cooled to 0 °C, and fresh anhydrous $AlCl_3$ (1.87 g, 14.07 mmol) was added. The reaction mixture was then stirred at 0 °C for 4 h, 30 °C for 8 h, 40 °C for 12 h, 60 °C for 12 h, and 80 °C for 24 h to obtain a dark-colored polymerized solid suspension. The resulting solid suspension was quenched using 50 mL of a HCl-H_2O mixture (*v*/*v* = 2:1), washed with water thrice and with ethanol twice, then with THF, methanol, water, acetone, pentane, and ether (100 mL each). It was further purified by Soxhlet extraction with 1:1 methanol/THF for 48 h, and then dried in a vacuum oven at 80 °C for 24 h to obtain a dark green solid. FTIR: (cm^{-1}) 2931, 2854, 1608, 1465, 1392, 1334, 1226, 1080, 1049, 879, 825, 748.

3.5. Synthesis of [POP-Pc′Cr(III)]][Co(CO)$_4$]

Inside the glove box, the heterogenized POP-Pc′Cr(III)Cl (1.00 g) was suspended in 10 mL dry THF and was added to a THF solution of $KCo(CO)_4$ (1.02 g). The solution was stirred at room temperature for 48 h, following which the reaction mixture was filtered to remove the dark precipitate, which was washed with THF (3 × 50 mL) and dried under high vacuum for 8 h to yield a dark green solid. FTIR: (cm^{-1}) 2965, 2870, 1882, 1608, 1458, 1396, 1334, 1218, 1080, 1053, 1049, 879, 825, 748.

3.6. PO Carbonylation Procedure

A stainless steel carbonylation reactor was dried overnight and placed inside the glove box. The reactor was charged with the POP-Pc′Cr(III)$Co(CO)_4$ catalyst (0.01 g, 12.16 μmol) and a dimethoxyethane solution of propylene oxide (1.8 M in 2.5 mL, PO/catalyst ratio = 200). The reactor was tightened completely and pressurized to 6 MPa of CO after the removal from the glove box and then placed in a preheated oil bath at 60 °C for 24 h. At 60 °C, the pressure was 6.2 MPa; after completion

of the reaction, the reactor was brought to room temperature (pressure ~6 MPa) and cooled in an ice bath, following which CO gas was vented slowly inside the fume hood. The filtrate of the reaction mixture was analyzed by ^{1}H NMR spectroscopy using internal standard naphthalene (*Caution*: carbon monoxide (CO) is a highly toxic gas, should be handled with extreme care inside the well-ventilated hood with a proper CO detector).

4. Conclusions

A new design strategy was presented for the facile synthesis of a chromium(III)phthalocyanine-based porous organic polymer (POP-Pc'CrCl) through a solvent-knitting Friedel–Crafts reaction. The constructed POP-Pc'CrCl has a high porosity with a BET specific surface area of 725 m^2 g^{-1}. When functionalized with cobaltate ($[Co(CO)_4]^-$) anions, the resulting heterogenized bimetallic Lewis acid–base ion pair catalyst exhibits epoxide ring-expansion carbonylation activity comparable to that of its homogeneous counterpart with slightly reduced activity during successive recycles which can be replenished upon catalyst regeneration. This new design strategy is useful for the synthesis of soluble metallophthalocyanines and one step construction of porous organic polymer for specific catalytic applications.

Supplementary Materials: The following are available online at http://www.mdpi.com/2073-4344/10/8/905/s1. Figure S1: ^{1}H NMR spectrum of ligand **1** measured in $CDCl_3$. Figure S2: ^{13}C NMR spectrum of ligand **1** measured in $CDCl_3$. Figure S3: UV-Visible spectrum of Pc'Cr(III)Cl (**2**). Figure S4: HR-MS of Pc'Cr(III)Cl (**2**). Figure S5: SEM and EDS mapping images of **3**. Figure S6: TEM images of **3**. Figure S7: Powder X-ray diffraction pattern of **3**. Figure S8: TGA plots of **2** and **3**. Figure S9: BJH pore size distribution graph of **3** and **4**.. Figure S10: SEM and EDS mapping images of **4**. Figure S11: TEM and EDS mapping images of **4**. Figure S12: SEM-EDS images of catalyst **4** after cycle three.

Author Contributions: V.G. and S.Y. designed the experiments. V.G. conducted the experiments. V.G. and S.Y. wrote the original draft. Review and edited by S.Y. Supervision, project administration, and funding acquisition by S.Y. All authors have read and agreed to the published version of the manuscript.

Funding: This work was supported by the C1 Gas Refinery Program (No. 2018M3D3A1A01018006) and ERC program (No. 2020R1A5A1018052) through the National Research Foundation of Korea (NRF) grants funded by the Ministry of Science, ICT and Future Planning, Republic of Korea.

Acknowledgments: We acknowledge the financial support by the C1 Gas Refinery Program (No. 2018M3D3A1A01018006) and ERC program (No. 2020R1A5A1018052) through the National Research Foundation of Korea (NRF) grants funded by the Ministry of Science, ICT and Future Planning, Republic of Korea.

Conflicts of Interest: The authors declare no conflict of interest.

References

1. Dunn, E.W.; Lamb, J.R.; Lapointe, A.M.; Coates, G.W. Carbonylation of Ethylene Oxide to β-Propiolactone: A Facile Route to Poly(3-hydroxypropionate) and Acrylic Acid. *ACS Catal.* **2016**, *6*, 8219–8223. [CrossRef]
2. Rajendiran, S.; Park, G.; Yoon, S. Direct Conversion of Propylene Oxide to 3-Hydroxy Butyric Acid Using a Cobalt Carbonyl Ionic Liquid Catalyst. *Catalysts* **2017**, *7*, 228. [CrossRef]
3. Getzler, Y.D.Y.L.; Kundnani, V.; Lobkovsky, E.B.; Coates, G.W. Catalytic Carbonylation of β-Lactones to Succinic Anhydrides. *J. Am. Chem. Soc.* **2004**, *126*, 6842–6843. [CrossRef] [PubMed]
4. Robinson, S.L.; Christenson, J.K.; Wackett, L.P. Biosynthesis and chemical diversity of β-lactone natural products. *Nat. Prod. Rep.* **2019**, *36*, 458–475. [CrossRef]
5. Wang, Y.C.; Tennyson, R.L.; Romo, D. β-lactones: Intermediates for Natural Product Total Synthesis and New Transformations. *Heterocycles* **2004**, *64*, 605–658. [CrossRef]
6. Li, Z.; Yang, J.; Loh, X.J. Polyhydroxyalkanoates: Opening doors for a sustainable future. *NPG Asia Mater.* **2016**, *8*, e265. [CrossRef]
7. Jiang, J.; Rajendiran, S.; Piao, L.; Yoon, S. Base Effects on Carbonylative Polymerization of Propylene Oxide with a [(salph)Cr(THF)2]+[Co(CO)4](-) Catalyst. *Top. Catal.* **2017**, *60*, 750–754. [CrossRef]
8. Rajendiran, S.; Gunasekar, G.H.; Yoon, S. A heterogenized cobaltate catalyst on a bis-imidazolium-based covalent triazine framework for hydroesterification of epoxides. *New J. Chem.* **2018**, *42*, 12256–12262. [CrossRef]

9. Rajendiran, S.; Park, K.; Lee, K.; Yoon, S. Ionic-Liquid-Based Heterogeneous Covalent Triazine Framework Cobalt Catalyst for the Direct Synthesis of Methyl 3-Hydroxybutyrate from Propylene Oxide. *Inorg. Chem.* **2017**, *56*, 7270–7277. [CrossRef]
10. Kramer, J.W.; Rowley, J.M.; Coates, G.W. Ring-Expanding Carbonylation of Epoxides. In *Organic Reactions*; Denmark, S.E., Ed.; Wiley: Hoboken, NJ, USA, 2015; pp. 1–104.
11. Getzler, Y.D.Y.L.; Mahadevan, V.; Lobkovsky, E.B.; Coates, G.W. Synthesis of β-Lactones: A Highly Active and Selective Catalyst for Epoxide Carbonylation. *J. Am. Chem. Soc.* **2002**, *124*, 1174–1175. [CrossRef]
12. Kramer, J.W.; Lobkovsky, E.B.; Coates, G.W. Practical β-Lactone Synthesis: Epoxide Carbonylation at 1 atm. *Org. Lett.* **2006**, *8*, 3709–3712. [CrossRef] [PubMed]
13. Schmidt, J.A.R.; Mahadevan, V.; Getzler, Y.D.Y.L.; Coates, G.W. A Readily Synthesized and Highly Active Epoxide Carbonylation Catalyst Based on a Chromium Porphyrin Framework: Expanding the Range of Available β-Lactones. *Org. Lett.* **2004**, *6*, 373–376. [CrossRef] [PubMed]
14. Schmidt, J.A.R.; Lobkovsky, E.B.; Coates, G.W. Chromium (III) Octaethylporphyrinato Tetracarbonylcobaltate: A Highly Active, Selective, and Versatile Catalyst for Epoxide Carbonylation. *J. Am. Chem. Soc.* **2005**, *127*, 11426–11435. [CrossRef] [PubMed]
15. Park, H.D.; Dincă, M.; Román-Leshkov, Y. Heterogeneous Epoxide Carbonylation by Cooperative Ion-Pair Catalysis in $Co(CO)4^-$-Incorporated Cr-MIL-101. *ACS Central Sci.* **2017**, *3*, 444–448. [CrossRef]
16. Rajendiran, S.; Natarajan, P.; Yoon, S. A covalent triazine framework-based heterogenized Al-Co bimetallic catalyst for the ring-expansion carbonylation of epoxide to beta-lactone. *RSC Adv.* **2017**, *7*, 4635–4638. [CrossRef]
17. Jiang, J.; Yoon, S. A Metalated Porous Porphyrin Polymer with $[Co(CO)4]^-$ Anion as an Efficient Heterogeneous Catalyst for Ring Expanding Carbonylation. *Sci. Rep.* **2018**, *8*, 13243. [CrossRef]
18. Ganesan, V.; Yoon, S. Hyper-Cross-Linked Porous Porphyrin Aluminum(III) Tetracarbonylcobaltate as a Highly Active Heterogeneous Bimetallic Catalyst for the Ring-Expansion Carbonylation of Epoxides. *ACS Appl. Mater. Interfaces* **2019**, *11*, 18609–18616. [CrossRef]
19. Ganesan, V.; Yoon, S. Direct Heterogenization of Salphen Coordination Complexes to Porous Organic Polymers: Catalysts for Ring-Expansion Carbonylation of Epoxides. *Inorg. Chem.* **2020**, *59*, 2881–2889. [CrossRef]
20. Rajendiran, S.; Ganesan, V.; Yoon, S. Balancing between Heterogeneity and Reactivity in Porphyrin Chromium-Cobaltate Catalyzed Ring Expansion Carbonylation of Epoxide into β-Lactone. *Inorg. Chem.* **2019**, *58*, 3283–3289. [CrossRef]
21. Jiang, J.; Rajendiran, S.; Yoon, S. Double Ring-Expanding Carbonylation Using an In Situ Generated Aluminum Phthalocyanine Cobalt Carbonyl Complex. *Asian J. Org. Chem.* **2018**, *8*, 151–154. [CrossRef]
22. Rowley, J.M.; Lobkovsky, E.B.; Coates, G.W. Catalytic Double Carbonylation of Epoxides to Succinic Anhydrides: Catalyst Discovery, Reaction Scope, and Mechanism. *J. Am. Chem. Soc.* **2007**, *129*, 4948–4960. [CrossRef] [PubMed]
23. Church, T.L.; Getzler, Y.D.; Byrne, C.M.; Coates, G.W. Carbonylation of heterocycles by homogeneous catalysts. *Chem. Commun.* **2007**, *7*, 657–674. [CrossRef] [PubMed]
24. Chao, C.-G.; Bergbreiter, D.E. Highly organic phase soluble polyisobutylene-bound cobalt phthalocyanines as recyclable catalysts for nitroarene reduction. *Catal. Commun.* **2016**, *77*, 89–93. [CrossRef]
25. Ghani, F.; Kristen, J.; Riegler, H. Solubility Properties of Unsubstituted Metal Phthalocyanines in Different Types of Solvents. *J. Chem. Eng. Data* **2012**, *57*, 439–449. [CrossRef]
26. Bulgakov, B.A.; Sulimov, A.V.; Babkin, A.V.; Kepman, A.V.; Malakho, A.P.; Avdeev, V.V. Dual-curing thermosetting monomer containing both propargyl ether and phthalonitrile groups. *J. Appl. Polym. Sci.* **2017**, *134*, 44786. [CrossRef]
27. Lever, A. The Phthalocyanines. In *Advances in Inorganic Chemistry and Radiochemistry*; Emeléus, H.J., Sharpe, A.G., Eds.; Academic Press: Cambridge, MA, USA, 1965; Volume 7, pp. 27–114.
28. Lee, W.; Yuk, S.B.; Choi, J.; Jung, D.H.; Choi, S.-H.; Park, J.; Kim, J.P. Synthesis and characterization of solubility enhanced metal-free phthalocyanines for liquid crystal display black matrix of low dielectric constant. *Dye. Pigment.* **2012**, *92*, 942–948. [CrossRef]
29. Padmanaban, S.; Yoon, S. Surface Modification of a MOF-based Catalyst with Lewis Metal Salts for Improved Catalytic Activity in the Fixation of CO_2 into Polymers. *Catalysts* **2019**, *9*, 892. [CrossRef]

30. Donohue, M.; Aranovich, G. A new classification of isotherms for Gibbs adsorption of gases on solids. *Fluid Phase Equilibria* **1999**, *158*, 557–563. [CrossRef]
31. He, W.-L.; Wu, C. Incorporation of Fe-phthalocyanines into a porous organic framework for highly efficient photocatalytic oxidation of arylalkanes. *Appl. Catal. B: Environ.* **2018**, *234*, 290–295. [CrossRef]
32. McKeown, N.B.; Makhseed, S.; Budd, P.M. Phthalocyanine-based nanoporous network polymers. *Chem. Commun.* **2002**, 2780–2781. [CrossRef]
33. Maffei, A.V.; Budd, P.M.; McKeown, N.B. Adsorption Studies of a Microporous Phthalocyanine Network Polymer. *Langmuir* **2006**, *22*, 4225–4229. [CrossRef] [PubMed]
34. Neti, V.S.P.K.; Wang, J.; Deng, S.; Echegoyen, L. High and selective CO_2 adsorption by a phthalocyanine nanoporous polymer. *J. Mater. Chem. A* **2015**, *3*, 10284–10288. [CrossRef]
35. Ma, P.; Lv, L.; Zhang, M.; Yuan, Q.; Cao, J.; Zhu, C. Synthesis of catalytically active porous organic polymer from iron phthalocyanine and diimide building blocks. *J. Porous Mater.* **2015**, *22*, 1567–1571. [CrossRef]
36. Xue, Q.; Xu, Z.; Jia, D.; Li, X.; Zhang, M.; Bai, J.; Li, W.; Zhang, W.; Zhou, B.; Wang, J. Solid-Phase Synthesis Porous Organic Polymer as Precursor for Fe/Fe_3 C-Embedded Hollow Nanoporous Carbon for Alkaline Oxygen Reduction Reaction. *ChemElectroChem* **2019**, *6*, 4491–4496. [CrossRef]
37. Ganji, P.; Doyle, D.J.; Ibrahim, H. In situ Generation of the Coates Catalyst: A Practical and Versatile Catalytic System for the Carbonylation of meso-Epoxides. *Org. Lett.* **2011**, *42*, 3142–3145. [CrossRef] [PubMed]
38. Kim, M.H.; Song, T.; Seo, U.R.; Park, J.E.; Cho, K.; Lee, S.M.; Kim, H.; Ko, Y.-J.; Chung, Y.K.; Son, S.U. Hollow and microporous catalysts bearing Cr(III)–F porphyrins for room temperature CO_2 fixation to cyclic carbonates. *J. Mater. Chem. A* **2017**, *5*, 23612–23619. [CrossRef]
39. Deng, F.-G.; Hu, B.; Sun, W.; Chen, J.; Xia, C. Novel pyridinium based cobalt carbonyl ionic liquids: Synthesis, full characterization, crystal structure and application in catalysis. *Dalton Trans.* **2007**, 4262–4267. [CrossRef]
40. Edgell, W.F.; Lyford, J. Preparation of sodium cobalt tetracarbonyl. *Inorg. Chem.* **1970**, *9*, 1932–1933. [CrossRef]